Appl. Phys. B 64, 567–572 (1997)

Applied Physics B Lasers and Optics

Precise measurement of methane in air using diode-pumped 3.4-μm difference-frequency generation in PPLN

K.P. Petrov[1], S. Waltman[2], E.J. Dlugokencky[3], M. Arbore[4], M.M. Fejer[4], F.K. Tittel[1], L.W. Hollberg[2]

[1] Rice Quantum Institute, Rice University, Houston, TX 77251-1892, USA
(Fax: +1-713/524-5237, E-mail: fkt@rice.edu)
[2] National Institute of Standards and Technology, Boulder, CO 80303, USA
(Fax: +1-303/497-7845)
[3] National Oceanic and Atmospheric Administration, Climate Monitoring and Diagnostics Laboratory, Boulder, CO 80303, USA
(Fax: +1-303/497-6975)
[4] Edward L. Ginzton Laboratory, Stanford University, Stanford, CA 94305-4085, USA
(Fax: +1-415/723-2666)

Received: 2 October 1996

Abstract. Fast, accurate measurement of the methane mixing ratio in natural air samples using a compact solid-state 3.4-μm difference-frequency spectrometer is reported. The spectrometer employed bulk periodically poled lithium niobate (PPLN) pumped by a solitary diode laser at 808 nm and a diode-pumped monolithic ring Nd:YAG laser at 1064 nm, and a 300 cm^3 volume multi-pass absorption cell with an 18-m path length. The methane mixing ratio was determined by comparing the direct optical absorption measured in the sample with that measured in a reference gas at 100 torr and room temperature. Relative accuracy of better than 1 ppb (parts in 10^9, by mole fraction) was achieved in measurements of natural air that contained 1700–1900 ppb methane. The typical measurement time for each sample was 60 seconds. The accuracy was limited by residual interference fringes in the multi-pass cell that resulted from scattering. Without the use of reference samples, the relative accuracy was 20 ppb; it was limited by the long-term reproducibility of the spectroscopic baseline, which was affected by drift in the optical alignment coupled to changes in the ambient temperature. This work demonstrates the use of diode-pumped difference-frequency generation (DFG) in PPLN in a high-precision infrared spectrometer. Compact, room-temperature solid-state gas sensors can be built based on this technology, for accurate real-time measurements of trace gases in the 3–5 μm spectroscopic region.

PACS: 07.65; 33.00; 42.60; 42.65; 42.80

Precise measurements of the global distribution of trace greenhouse gases such as CH_4, CO_2, and N_2O provide some of the best-known constraints on their global budgets, i.e. sources to, and removal from, the atmosphere. For example, the NOAA Climate Monitoring and Diagnostics Laboratory (CMDL) operates a globally distributed network of surface air sampling sites from which more than 7000 air samples are analyzed for CH_4 each year [1]. The current measurement technique, gas chromatography (GC), is robust and precise (with a relative precision of $\sim 0.1\%$), but it is slow, requiring approximately 15 minutes for each measurement. Expansion of the sampling network at the surface into the vertical, a necessary step to better constrain the global CH_4 budget [2], would overwhelm the current analysis capacity.

Infrared laser spectroscopy is a uniquely effective method for the measurement of trace gas concentrations because it combines high precision, remote sensing capabilities, and fast response. These features can benefit applications in which many gas samples are analyzed or time-dependent changes in gas concentration are monitored. Several instruments have been developed based on lead-salt diode lasers that offer detection sensitivities down to 0.05 ppb (parts in 10^9, by mole fraction) for several trace species in air at atmospheric or reduced pressure [3–5]. However, lead-salt diode lasers require cooling to liquid nitrogen temperatures, have problems with mode jumps and multi-mode operation, and often require a large monochromator for mode selection, which in many applications are considerable disadvantages. The need for cryogenic cooling can potentially be eliminated in infrared spectrometers based on InAsSb [6] and InGaAsSb [7] semiconductor lasers, which have recently seen considerable development. They hold the promise of potential single-frequency operation with output powers in excess of 1 mW at temperatures that can be reached with Peltier coolers. However, single-frequency, single-spatial-mode lasers are not currently available. An attractive alternative to mid-infrared diode lasers is difference-frequency generation (DFG). Difference-frequency mixing of Ar^+ and dye [8], also dye and Ti:Al_2O_3 [9] lasers was effectively used for high-resolution infrared spectroscopy of stable molecules and short-lived free radicals. Several feasibility tests have recently indicated that DFG-based spectrometers pumped by commercial near-infrared diode lasers can cover most of the spectroscopic fingerprint region from 3 to 18 μm. In particular, typical linewidths of less than 50 MHz and output powers from 0.5 to 30 μW have been reported for diode-pumped DFG sources operating near 3 μm [10], 4 μm [11], 5 μm [12], and 9 μm [13]. In these experiments, spectroscopic measurements of methane and carbon monoxide in natural air have indicated that detector-limited sensitivity can be achieved, corresponding to minimum detectable column densities of less than 10 ppb m $(Hz)^{-1/2}$. Waveguide DFG sources hold promise for

higher output powers, but no practical spectroscopic system has yet been reported.

The purpose of this work was to design and test an all-solid-state room-temperature IR spectrometer for fast measurement of atmospheric methane with a precision of < 1 ppb, and to investigate the long-term stability of its calibration. We report the operation of such a compact spectrometer, based on quasi-phase-matched DFG at 3.4 µm in bulk periodically poled lithium niobate (PPLN) pumped by a solitary diode laser and a diode-pumped Nd:YAG laser. The spectrometer was used for measurements of the methane mixing ratio in natural air samples with < 1 ppb relative accuracy with signal averaging time of 60 seconds. This is the first reported application of PPLN in a high-precision infrared spectrometer.

1 Experimental setup

Figure 1 shows a schematic diagram of the DFG spectrometer used for CH_4 measurement from natural air samples. It employed two compact laser sources: a 100 mW solitary Fabry–Perot diode laser at 808 nm (pump) and a 500 mW diode-pumped monolithic ring Nd:YAG laser at 1064 nm (signal). The single-frequency outputs of these two lasers were mode-matched, combined by a dichroic beamsplitter, and focused into an uncoated PPLN crystal. The 10 mm-by-10 mm crystal was cut from a 0.5-mm-thick wafer of lithium niobate with a 21 µm periodic domain grating fabricated by electric field poling [14]. The input facets were cut 13° relative to the grating lines, making it possible to use effective grating periods between 21 µm and 24 µm with external incidence angles below 35°. This configuration allows room-temperature generation of 3–5 µm radiation by mixing near-infrared diode lasers with a Nd:YAG laser at 1064 nm while using the largest nonlinear coefficient in lithium niobate, $d_{33} = 27\ \mathrm{pm\,V^{-1}}$, for mixing three extraordinarily polarized waves. Quasi-phase-matched generation of 3.35 µm radiation (idler) was achieved by using an effective grating period of 22.2 µm, with an external incidence angle of 13.2°.

The idler was collimated by an uncoated CaF_2 lens. With 70 mW of diode power at 808 nm and 500 mW Nd:YAG power at 1064 nm incident on the uncoated mixing crystal, a maximum of 3.4 µW idler power was measured. Because the PPLN crystal was oriented such that the incident beams propagated at an angle with respect to the grating *k*-vector, a walkoff between the idler beam and the incident beams limited the interaction length to approximately 7 mm. This phase-velocity walkoff [15] effect, analogous to Poynting vector walkoff in birefringent materials, could be avoided by using a 22.2-µm grating period at incidence close to normal.

Approximately 40% of the IR output was deflected by an uncoated ZnSe wedge and measured at a liquid-nitrogen-cooled InSb detector. The beam transmitted through the wedge was focused into a multi-pass absorption cell which provided an 18 m optical path length with 90 passes through the sample volume of 300 cm^3. The cell had a tilted BaF_2 window and a measured optical throughput of 41% which corresponds to a mirror reflectance of 99.1%. The cell was connected to a rotary pump and a manifold that allowed switching between two high-pressure aluminum cylinders containing natural air that had been previously calibrated for methane at CMDL. The pressure in the cell was maintained near 100 torr, as measured by a capacitive manometer with 0.01 torr resolution and 0.2 torr accuracy. The cell temperature was measured using a mercury thermometer with 0.1 °C resolution. After the cell, the DFG beam was collected by an off-axis parabol-

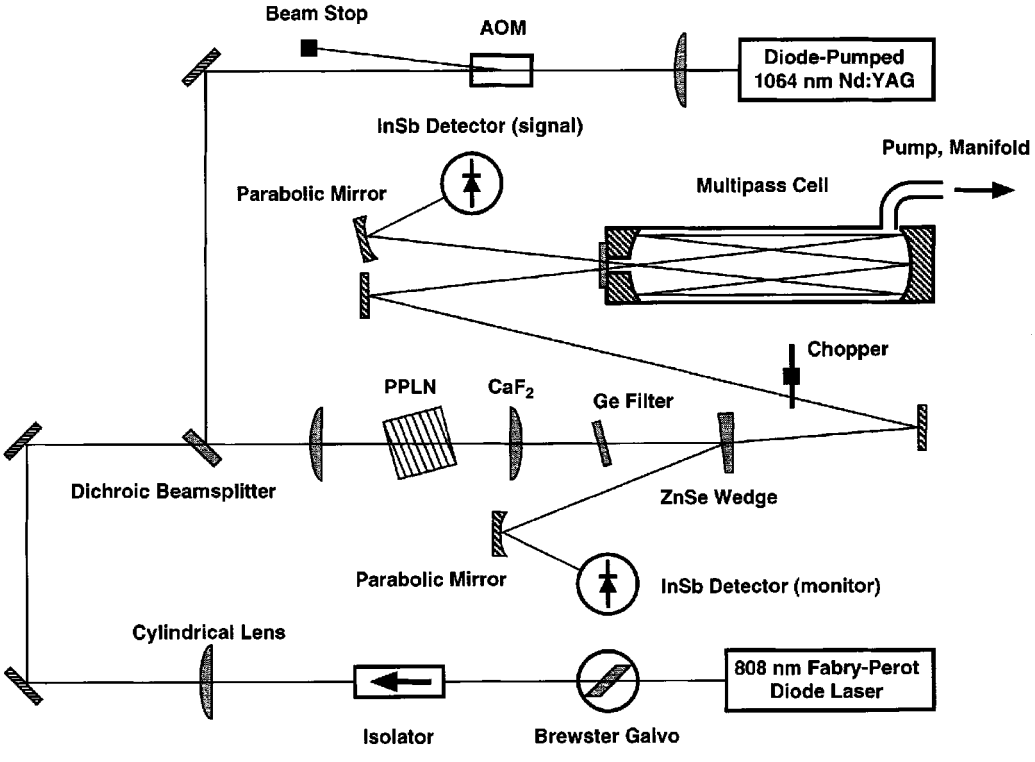

Fig. 1. Schematic diagram of a compact 3.4 µm spectrometer based on bulk PPLN pumped by two solid-state lasers. The spectrometer was used to measure the methane mixing ratio in natural air at 100 torr and room temperature relative to a reference gas to better than 1 ppb in 60 seconds

ic mirror and focused onto a second liquid-nitrogen-cooled InSb detector with a $1 \times 1\,\mathrm{mm}^2$ active area. The detector had a noise-equivalent power (NEP) of $1.7\,\mathrm{pW\,(Hz)}^{-1/2}$ at $3.4\,\mu\mathrm{m}$.

2 Reduction of interference and noise

In addition to the basic elements described above, several other components were required to improve the output stability and tuning characteristics of the DFG spectrometer. Initial measurements showed that the linearity of the frequency sweep of the pump laser was degraded by weak optical feedback from scattering in the optical isolator. This resulted in distortion of the observed spectral lineshapes and an unstable baseline profile. To reduce the unwanted distortion, a galvo-driven Brewster plate [16] was placed in the diode laser beam before the isolator. The Brewster plate was rocked at 5 Hz to scramble the phase of the optical feedback. This did not remove the feedback, but it did ensure a reproducible baseline for absorption spectra which were averaged over many scans.

We observed alignment-dependent optical interference fringes in the multi-pass absorption cell. They were caused by scattering from beam spots in close proximity to the output window at the center of the front mirror. The smallest magnitude of these fringes was approximately 5×10^{-4} absorption units. To cancel the fringes, a voice coil was attached to the cell. The coil was driven by a sine-wave generator tuned to an acoustic resonance in the cell near 800 Hz. Vibration of the cell mirrors resulted in an excursion of fringes that was larger than their period. This reduced the magnitude of the interference in the averaged absorption signal by more than a factor of 10. No evidence of drift in the alignment of the cell mirrors was found during 5 weeks of experiment.

The commercial InSb detector that sampled the DFG power before the multi-pass absorption cell was modified to have a 77 K quartz filter and an aperture. The dc-coupled detector output was subtracted from a precision voltage reference, and the filtered error signal was used to control an acousto-optic modulator placed in the Nd:YAG beam. This servo removed amplitude modulation associated with frequency scans, beam offset caused by motion of the Brewster plate, acoustic vibration, and alignment drift. However, since the servo-stabilized output of the monitor detector includes dark voltage, the output DFG power still changed as the dark voltage changed with temperature. Temperature stabilization of the entire system, including the background seen by the monitor detector, could improve the power stability. After the wedge beamsplitter, the IR beam path to the first detector was nearly equal to the beam path outside the multi-pass cell to the second detector, making it possible to cancel out absorption by methane in ambient air. Considering that temporal fluctuations of the methane concentration in room air can easily exceed 10%, improper cancellation of stray absorption would result in signal errors that are unacceptable in this precision application. Nitrogen-purging of the spectrometer would further reduce stray absorption caused by spatial fluctuations of methane concentration.

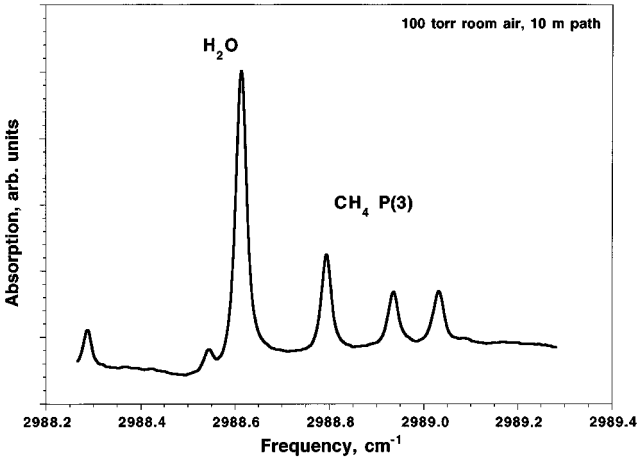

Fig. 2. Survey absorption spectrum of room air near 3.35 μm at 100 torr in a 10-m multi-pass cell. The observed transitions belong to water (2988.6 cm^{-1} and lower) and the P(3) group of methane (2988.8 cm^{-1} and higher). The trace shown is a 1024-sweep average with baseline subtracted. The sweep rate was 100 Hz

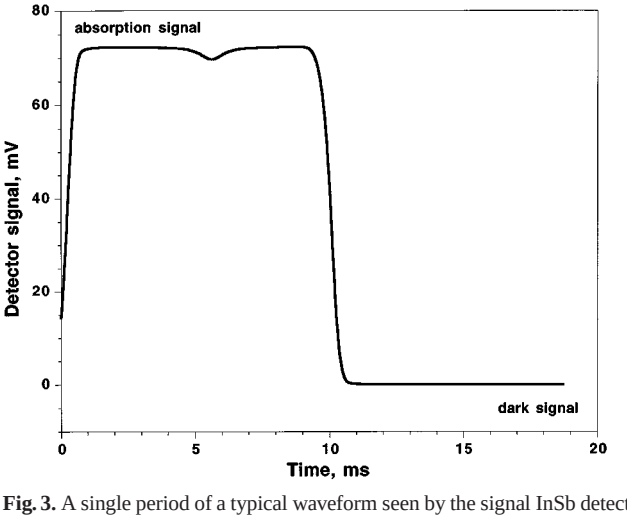

Fig. 3. A single period of a typical waveform seen by the signal InSb detector. A direct-absorption spectrum of an isolated methane line was recorded during the first 10 ms. Over the next 10 ms, the beam was blocked by the chopper and the dark voltage was recorded. The average of the dark voltage was subtracted from the entire trace

3 Control and measurement

The temperature of the Fabry–Perot diode laser was stabilized for operation with a center wavelength of 808 nm. Fine wavelength tuning and scans were performed by modulation of the laser drive current. The maximum available fine-tuning range of 35 GHz without mode-hops was sufficient for simultaneous observation of several strong molecular transitions of methane and water (Fig. 2). For absorption measurements, a tuning range of 7 GHz was adequate to capture a single methane peak. The DFG signal detected after the multi-pass absorption cell was low-pass filtered below 10 kHz and digitized by a 16-bit analog-to-digital converter. The frequency sweep was triggered by a 50 Hz chopper, such that the IR beam was blocked during retrace of the frequency sweep. This arrangement permitted sampling of the signal detector's dark voltage and the absorption trace during each sweep cycle, as seen in Fig. 3. The 50 Hz sweep rate was chosen to combine

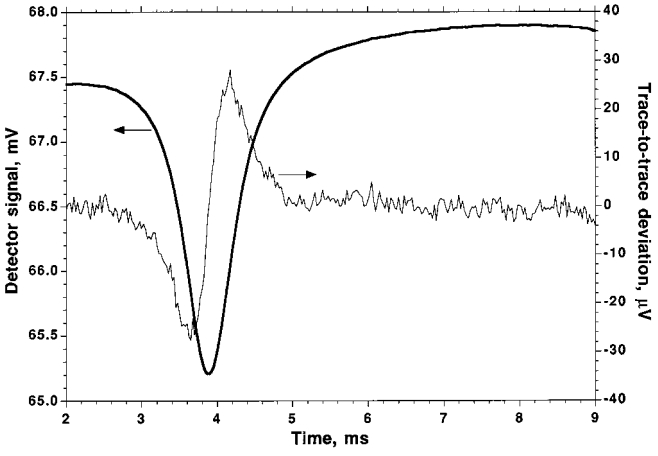

Fig. 4. A close-up of an absorption peak (thick solid line) similar to that shown in Fig. 3. The thin solid trace in the middle is the difference between absorption traces acquired 5 minutes apart. Detector noise can be seen in the flat part of the trace. The anti-symmetric feature is a result of frequency drift

minimal distortion of the signal by the 10 kHz low-pass filter and reasonably short measurement time.

Each measurement consisted of a 3000 sweep average acquired over 60 seconds. An example of such measurement—a trace of detector voltage versus time—is shown in Fig. 4. The thick solid trace was acquired with the use of cancellation of interference fringes in the multi-pass cell. The thin solid line is the difference between two such traces acquired 5 minutes apart. The preamplifier had a single-pole low-pass filter with a 3 dB corner frequency of 10 kHz. The equivelant noise bandwidth of the average of 3000 sweeps was 5.2 Hz. Infrared detector noise measured in this bandwidth corresponds to 8×10^{-6} rms absorption which can be easily observed in the thin trace because of the large dynamic range ($16+11$ bits) available in the averaged signal. The peak amplitude was extracted from the absorption trace by using nonlinear least-squares fitting. Prior to fitting, the retrace average of the dark voltage was subtracted from the entire trace. The parameters of the fitting included the peak position, pressure- and Doppler-broadened linewidths $\Delta\nu_p$ and $\Delta\nu_T$, and a linear fit to the baseline. Voigt line shape was assumed, and a rational approximation [17] was used to compute the normalized absorption profile. Absorption α was determined by normalizing the peak amplitude to the value of the fitted baseline taken at the center of the peak. Values of the absorption for the various calibrated air samples used in the experiment ranged between 3% and 4%. Corrected for total pressure and temperature, T, of each sample, the absorption was assumed to be proportional to the methane mole fraction in that sample [here $V(0;\Delta\nu_p/\Delta\nu_T)$ is the peak value of the normalized Voigt function]:

$$C \propto -T\ln(1-\alpha)V\left(0;\frac{\Delta\nu_p}{\Delta\nu_T}\right).$$

Such correction was necessary because the cell temperature was observed to change by more than 1 °C during the experiment, and the fill-to-fill variations in sample pressure were as large as 0.5 torr. The constant of proportionality is omitted in the above formula, since it depends on quantities such as the line intensity and optical path length – each known to ±2%, at best. The sample pressure and pressure-broadening coefficient, both known to better than ±0.2%, are included in the above formula in the form of $\Delta\nu_p$, and their combined effect on the value of the normalized Voigt function is less than 0.04%. Initially, an attempt was made to determine the constant of proportionality in the above formula. With the use of a single air sample with known methane mixing ratio this should be possible, and the result could be used to measure CH_4 from other samples. We have found, however, that the day-to-day reproducibility of the spectroscopic baseline, which depended on alignment and was strongly coupled to changes in ambient temperature, limited the accuracy of such measurement to about 1%. This demonstrated that measurements with 1% absolute accuracy would be possible, and in many cases such accuracy is more than adequate. However, our specific application required precision of better than 0.1%. We have therefore resorted to using a reference sample before (or after) each unknown sample. This is a somewhat less attractive technique because it requires an additional gas transfer and roughly doubles the measurement time. In some applications, however, this is acceptable and could be used to verify whether the instrument is working properly. It is important to point out that this technique does not solve the problem of baseline drift; it only makes the drift insignificant on the time scale of an individual measurement.

4 Performance testing and results

The performance of the DFG spectrometer was tested by using four high-pressure aluminum cylinders filled with dry air, as supplied by NOAA CMDL. All four cylinders had been calibrated for methane at CMDL via gas chromatography. The precision of the measurements was typically better than 1 ppb, and methane mole fractions were assigned relative to the CMDL methane scale [1]. The testing was performed in two parts. In the first part, two cylinders (identification numbers 30516 and 37057) were supplied with their methane mole fractions. The second part was blind; the two authors performing the spectroscopic measurements (KPP and SW) were not told the methane mole fractions in the two other cylinders (64040 and 30482).

The methane mole fractions assigned to the cylinders used in the first test were 1775.3 ± 0.1 ppb for cylinder 30516 and 1896.7 ± 1.3 ppb for cylinder 37057. Air samples from each cylinder were analyzed continuously for 5 minutes, with a 15 minute pause between the samples. The pause was made to completely evacuate the multi-pass cell and to let the newly injected sample reach thermal equilibrium with the cell. These measurements were performed without cancellation of fringes in the cell. Figure 5 shows the measured absorption by methane as a function of time. The sample temperature of 25.0 ± 0.1 °C though not actively stabilized, was not observed to change in this test. When corrected for differences in the sample pressure as explained above, the ratio of methane mole fractions is found to be 1.0681 ± 0.0015, versus 1.0684 ± 0.0007 as calculated from the gas chromatograph data. As suspected, the primary source of large deviations among individual measurements is interference fringes in the multi-pass absorption cell. Although weak, they still produced baseline features clearly distinguishable from detector noise, and they affected the precision

with which the fitting parameters were determined. Since no changes in the ambient temperature were observed during this test, the measurements were not affected by drift in optical alignment.

In the subsequent blind tests, cylinders 30482 and 64040 were analyzed. Cancellation of interference fringes in the multi-pass cell was used this time, as the need for it had been clearly realized. Measurements of optical absorption in cylinder 30482 relative to cylinder 30516 (reference) gave a methane mixing ratio of 1781.1 ± 0.8 ppb after correction for pressure and temperature (Fig. 6). The CH_4 mixing ratio assigned to that cylinder by CMDL was 1781.9 ± 0.9 ppb. A summary of data obtained for all samples analyzed in the experiment is given in Table 1. Since cylinder 30516 was used as a reference in all measurements, its methane mixing ratio of 1775.3 ppb was assumed to be known exactly. Therefore the uncertainty in the mixing ratio determined by CMDL is not included in the errors given for spectroscopic measurements. The errors quoted in Table 1 represent instead the combined uncertainties in the measured optical absorption, temperature, and pressure.

Table 1. Summary of methane mixing ratios measured using the 3.4 µm DFG spectrometer. Four samples were available in the experiment, and one of them (30516) was used as a reference in all measurements. The methane mixing ratio in this sample was assumed to be known exactly. Standard deviation shown for the DFG data therefore only includes errors of measurement of absorption, temperature, and pressure. Sample 37057 was measured without cancellation of interference in the multi-pass cell, hence the large error bar

cylinder identification number	CDML CH_4 assignment (ppb)	standard deviation (ppb)	3.4 µm DFG measurement (ppb)	standard deviation (ppb)
64040	1753.8	0.2	1754.3	0.8
30516	1775.3	0.1	used as areference	n/a
30482	1781.9	0.9	1781.1	0.8
37057	1896.7	1.3	1896.2	3.0

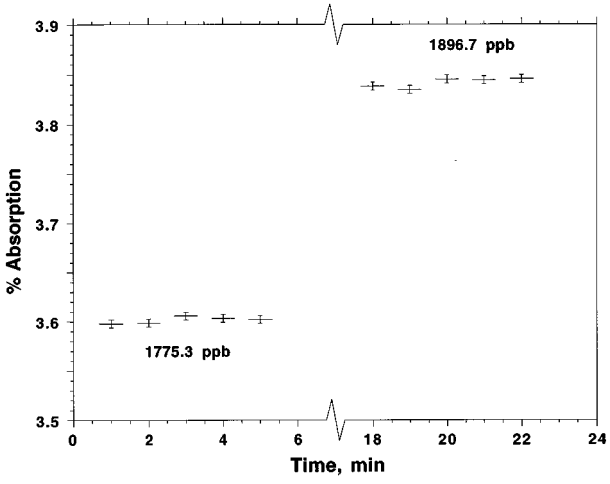

Fig. 5. Peak absorption by CH_4 versus time, measured for two air samples previously calibrated for methane (indicated on the plot). The measured ratio of mole fractions is 1.0681 ± 0.0015, after correction for differences in pressure. This can be compared with the ratio of 1.0684 ± 0.0007, determined from the CH_4 mole fractions assigned to the samples. Cancellation of interference was not used in this data, hence the large error bar

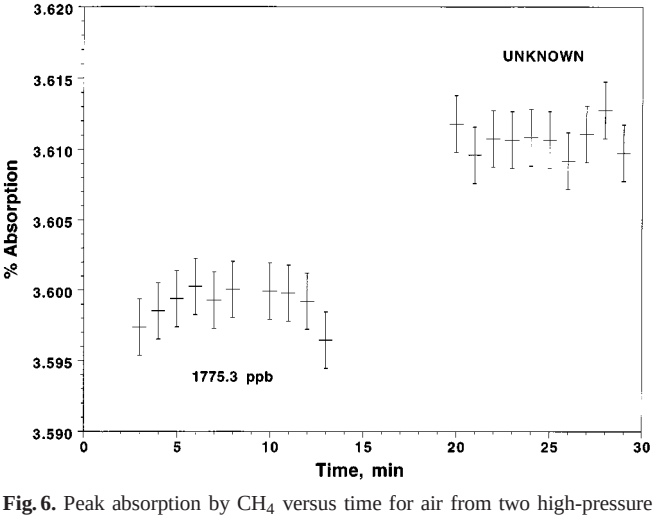

Fig. 6. Peak absorption by CH_4 versus time for air from two high-pressure cylinders. The 10 measurements plotted on the lower left from cylinder 30516 (with a CH_4 mole fraction of 1775.3 ppb assigned by CMDL) were used as a reference. The 10 measurements in the upper right were for cylinder 30482 which was analyzed as an unknown. The spectroscopic result for the unknown was 1781.1 ± 0.8 ppb; this compares well with the value of 1781.9 ± 0.9 ppb assigned by CMDL

The data suggest that the combined uncertainty of the spectroscopic measurements over 1 minute is less than 1 ppb for a typical ambient methane mixing ratio of 1700–1900 ppb. This is equivalent to about 0.06% rms relative accuracy. Taking into account the conditions of our experiment (18 m path length, 5.2 Hz bandwidth) we estimate the noise-equivalent methane column density of $6.3\ \text{ppb m}\,(\text{Hz})^{-1/2}$.

5 Summary

We have demonstrated a precise spectroscopic application of diode-pumped difference-frequency generation. A compact 3.4-µm spectrometer employed a 1-cm-long PPLN crystal with a 21-µm domain grating period, pumped by two compact solid-state lasers: a 100-mW solitary laser diode at 808 nm (pump), and a diode-pumped monolithic ring Nd:YAG laser at 1064.5 nm (signal). With a maximum total output power of 3.4 µW at 3.4 µm, the DFG source of the spectrometer performed continuous frequency scans of more than 35 GHz, and could be tuned over more than $60\ \text{cm}^{-1}$ by scanning the temperature the pump laser. The use of a galvo-driven Brewster plate allowed compensation of feedback distortion of the frequency sweep. Sampling and servo control of the output power allowed cancellation of the amplitude modulation and noise due to frequency sweep, acoustic noise, and alignment drift. The spectrometer employed a compact 18 m multi-pass cell which had an optical throughput of 41%.

The measurements were made relative to the CMDL standard methane scale. With a measurement time of 60 seconds, direct-absorption spectroscopy of methane in natural air samples was performed, and the methane mixing ratios were determined with a precision of better than 1 ppb. The precision was limited by residual interference fringes in the multi-pass cell. The peak-to-peak magnitude of the fringes corresponds to a signal-to-noise ratio of 510 for the meas-

ured optical absorption of $\sim 3.5\%$. Without a reference gas, the relative accuracy of 20 ppb was limited by the long-term stability and reproducibility of the spectroscopic baseline. The baseline profile depended on the optical alignment, which drifted following changes in the ambient temperature.

This precision spectrometer can benefit applications where many similar gas samples are analyzed. In trace-gas-monitoring applications that require fast measurements with an accuracy of down to 1%, such a spectrometer can employ room-temperature InAs infrared detectors and operate without reference samples. Diode-pumped DFG in PPLN can effectively replace lead-salt diode lasers and gas lasers in spectroscopic applications requiring low-noise, single-frequency sources that are continuously tunable in the 3–5 μm region, and eliminate the need for cryogenic cooling.

Acknowledgements. The authors are grateful to Charlie Hultgren of New Focus, Inc. and Richard Fox at NIST Boulder for helpful discussions. The work was supported in part by the NOAA Climate Monitoring and Diagnostics Laboratory, the National Aeronautics and Space Administration, the Advanced Research Projects Agency through the Center for Nonlinear Optical Materials at Stanford University, the Joint Services Electronics Program, the National Science Foundation, the Texas Advanced Technology Program, and the Robert A. Welch Foundation.

References

1. E.J. Dlugokencky, L.P. Steele, P.M. Lang, K.A. Masarie: J. Geophys. Res. **99**, 17021 (1994)
2. I. Fung, J. John, J. Lerner, E. Matthews, M. Prather, L.P. Steele, P.J. Fraser: J. Geophys. Res. **96**, 13033 (1991)
3. J. Reid, M. El-Sherbiny, B.K. Garside, E.A. Balik: Appl. Opt. **19**, 3349 (1980)
4. C.R. Webster, R.D. May, C.A. Trimble, R.G. Chave, J. Kendall: Appl. Opt. **33**, 454 (1994)
5. M.S. Zahniser, D.D. Nelson, J.B. McManus, P.L. Kebabian: Phil. Trans. R. Soc. Lond. A **351**, 371 (1995)
6. A. Popov, B. Scheumann, R. Mücke, A. Baranov, V. Sherstnev, Y. Yakovlev, P. Werle: Infrared Physics and Technology **37**, 117 (1996)
7. D.Z. Garbuzov, R.U. Martinelli, R.J. Menna, P.K. York, H. Lee, S.Y. Narayan, J.C. Connolly: Appl. Phys. Lett. **67**, 1346 (1995)
8. A.S. Pine: J. Opt. Soc. Am. **66**, 97 (1976)
9. C.E. Miller, W.C. Eckhoff, R.F. Curl: J. Mol. Struct. **352**, 435 (1995)
10. K.P. Petrov, S. Waltman, U. Simon, R.F. Curl, F.K. Tittel, E.J. Dlugokencky, L. Hollberg: Appl. Phys. B **61**, 553 (1995)
11. A. Balakrishnan, S. Sanders, S. DeMars, J. Webjörn, D.W. Nam, R.J. Lang, D.G. Mehuys, R.G. Waarts, D.F. Welch: Opt. Lett. **21**, 952 (1996)
12. K.P. Petrov, L. Goldberg, W.K. Burns, R.F. Curl, F.K. Tittel: Opt. Lett. **21**, 86 (1996)
13. K.P. Petrov, L. Goldberg, R.F. Curl, F.K. Tittel: Opt. Lett. **21**, 1451 (1996)
14. L.E. Myers, R.C. Eckardt, M.M. Fejer, R.L. Byer, W.S. Bosenberg, J.W. Pierce: J. Opt. Soc. Am. B **12**, 2102 (1995)
15. M.M. Fejer, G.A. Magel, D.H. Jundt, R.L. Byer: IEEE J. Quan. Elec. **28**, 2631 (1992)
16. C.R. Webster: J. Opt. Soc. Am. B **2**, 1464 (1985)
17. J. Humlicek: J. Quant. Spectrosc. Radiat. Transfer **21**, 309 (1979)